

Effects of Welding Position, Heat Treatments, and Surface Roughness on the Fatigue Behavior of Welded Aluminum Alloys Using Friction Stir Welding

Dr. Shaker Sakran Hassan

Machines and Equipment Engineering Department, University of Technology
Email: sadeqbakhy@yahoo.com

Dr. Sadeq Hussein Bakhy

Machines and Equipment Engineering Department, University of Technology

Athraa Ali Jawad

Machines and Equipment Engineering Department, University of Technology

Received on: 30/1/2014 & Accepted on: 4/9/2014

ABSTRACT

The present work is aimed to study the fatigue behavior of friction stir welding for the similar and dissimilar joints taking into account the effects of welding position, post welding heat treatments, and surface roughness. The materials were used AA2024T3 and AA6061T6. The maximum welding efficiency achieved at friction stir welding process was 62.8 % of the base metal for the similar 2024-T3 joint, and this value was improved by using post welding heat treatments and reach to 67.9%. Results showed that fatigue strength at 10^6 cycles depended strongly on welding line position where for welding line at a distance 0.35L from loading side, the reduction in fatigue limit with respect to 2024T3 base material was 45% for similar joint and 58% for dissimilar joints, and for welding line at a distance 0.7 L, the reduction in fatigue strength was 56% for similar joint and 67% for dissimilar joints. While, it was a large reduction in the fatigue strength reaching to 70% in both similar and dissimilar joint for the welding joint at a distance L (i.e at the fixing end). The heat treatments improved the fatigue strength about 31% more than non heat treatments of the similar 2024T3 joint by fsw at 0.7L in high cycle regime. Finally, the non-finishing samples showed a reduction in fatigue strength reaching to 10% more than the finishing samples of the similar 2024T3 joint at 0.7L.

Keywords: Friction stirs welding, Fatigue, Heat treatments, Surface roughness.

تأثيرات موقع اللحام, المعاملات الحرارية, وخشونة السطح على سلوك الكلال لسبائك
الألمنيوم الملحومة باستخدام لحام الخلط الأحتكاكي

الخلاصة

يهدف البحث الحالي الى دراسة تصرف الكلال للمفاصل المتماثلة والمتباينة الملحومة بلحام الخلط الأحتكاكي مع الأخذ بنظر الاعتبار تأثير موقع اللحام, المعاملات الحرارية للمفاصل الملحومة, وخشونة السطح. وقد استخدمت سبائك الألمنيوم 2024T3 و 6061T6. بينت النتائج ان أعلى كفاءة لحام وصلت الى 62.8% لمقطع ملحوم بمواد متشابهة (2024T3) و هذه القيمة ازدادت بعد اجراء المعاملات الحرارية لنفس المقطع ووصلت الى 67.9%. أظهرت النتائج أن مقاومة الكلال عند 10^6 من الدورات تعتمد بقوة على موقع خط اللحام

, اذ وجد ان مقاومة الكلال لخط لحام على بعد 0.35L من جهة تسليط القوة كانت 45% للمفاصل المتماثلة (2024T3- 2024T3) و 58% للمفاصل المتباينة (2024T3-6061T6) نسبة الى 2024T3 المادة الأساسية الغير ملحومة. وللعينات التي يكون خط اللحام فيها على بعد 0.7L كان الانخفاض في مقاومة الكلال 56% للمفاصل المتماثلة 67% للمفاصل متباينة. في حين، كان هناك انخفاض كبير في مقاومة الكلال تصل إلى 70% للمفاصل المتماثلة والمتباينة لموقع اللحام على مسافة L (اي عند نقطة التثبيت). تم تحسين مقاومة الكلال باستخدام المعاملات الحرارية لعينات 2024T3 المتماثلة الملحومة تصل إلى 31% عن نفس العينات التي لم يجرى لها معاملات حرارية. أخيراً، كان هناك انخفاض في مقاومة الكلال تصل 10% للعينات غير منعمة السطح لعينات 2024T3 المتماثلة من العينات المنعمة.

INTRODUCTION

Friction stir welding (FSW) is a promising welding process that can produce low-cost and high-quality joints; it is well suited for joining aluminum alloys, especially for those usually considered as un-weldable such as 2xxx and 7xxx series [1]. The maximum temperature measured during friction stir welding of materials falls between 0.7 and 0.9 of melting point. Figure (1) illustrates the FSW process [2]. Fatigue performance of the FS welded joints are presented in some workes. AA6082-T6 butt joints fatigue resistance by varying the most relevant process parameters were investigated [3]. The comparative study on fatigue properties between AA2024-T4 friction stir welds and base material with influenced zigzag-curve defects across weld section on the fatigue properties of FSW joints were studied [4]. Fatigue crack growth behavior of friction stir butt welds of 3 mm thick 6082-T6 aluminum alloy was introduced [5]. Fatigue crack growth curves were determined for cracks growing in different locations of the weld elements, namely the base material, friction stirred material and heat affected material. The effect of microstructure and post heat treatment on fatigue behavior of the dissimilar joints of cast aluminum alloy, AC4CH-T6, and wrought aluminum alloy, A6061-T6, by means of friction stir welding (FSW) technique were investigated [6]. The effect of peening on the fatigue crack growth performance of friction stir-welded 7075 aluminum alloy was studied [7]. The fatigue behaviors of single-sided friction stir butt welds in different welding conditions in 3 mm thick 3003-O non-heat treatable aluminum alloys were presented [8]. The fatigue at the optimum FSW result was tested then the results were compared with TIG and base metal [9]. Many tests were made to examine the results of welding, these tests were Tensile, Hardness, Bending, Fatigue, Micrographic, Crack propagation and, X-Ray. Laser peening was applied without coating (LPwC) to fatigue specimens cut out from friction stir welded A6061T6 aluminum alloy plates with a thickness of 3 mm. The effects on the fatigue properties were studied through plane bending fatigue tests with a stress ratio of $R = -1$ [10].

The friction stir welding process for the aluminum alloy 2024-T3 was studied [11]. The welding process was performed at different rotational speeds and variable feeding rates. It was obtained that the best result was in the forward welding travel and counter clockwise tool rotation. Also, the distribution of the microhardness was found to be similar to that of the first welding process in distribution. It was found that the maximum tensile strength reached in stir welding process was 72% of the base metal and didn't improve in the FS process.

Some of mechanical properties of friction stir welded joints were investigated for (7020-T53) aluminum alloy sample of 5 mm thickness [12]. Three types of tool geometry, four rotational speeds (710, 900, 1120 and 1400 rpm) and three travel

speeds (16, 25 and 40 mm/min) were used. The results showed that aluminum alloy (7020-T53) can be welded using (FSW) process with maximum welding efficiency (83%) in terms of ultimate tensile strength using the best welding parameters (1400 rpm) rotational speed and 40 mm/min travel speed. The three dimensional non-linear numerical model using ANSYS software was built. Numerical results of the residual stresses showed the conventional “M” profile. Natural frequencies of friction stir welded plate are lower than that of base metal plate.

From above, it is clear that a large number of the published researches that utilize friction stir welding concerned with the influence of the welding parameters (tool rotational speed and welding speed) and the tool geometry on the mechanical properties, residual stresses and microstructure of the friction stir welded joint. Other researches studied the temperature distribution along the welding line, but none of these references investigated the effect of welding position and the effect of softening and polishing on the fatigue behavior of friction stir welded joints. Therefore, the aim of the current work is to characterize the fatigue behavior of similar (2024-T3) and dissimilar (2024-T3, 6061-T6) friction stir welded joints at different position of welding. In addition to that, the work is concerned with the influence of the post welding heat treatments and the effect and polishing and softening for the similar 2024-T3 joint on the fatigue behavior and some of mechanical properties.

EXPERIMENTAL WORK

In this investigation, a rolled section of (3 mm) thick sheet of a heat treatable aluminum alloys 2024-T3 and 6061-T6 were used as received. The chemical compositions are listed in Table (1). The sheets were cut and machined into rectangular welding samples of 300mm long by 100mm wide. Every two samples were secured into a carbon steel backing plate using specially designed mechanical clamps to avoid separation or lateral movement from the joint line during the welding process. The welding samples were then longitudinally butt-welded perpendicular to sheet rolling direction using a vertical type milling machine. During the welding cycles, the tool was rotating in the clock-wise direction and was tilting 2 degrees with respect to a vertical axis. The tool has a small diameter entry probe or pin of 3 mm, and 2.8 mm length with a diameter shoulder of 10 mm, the welding Tool was made from tool steel as shown in Figure (2).

The downward pressure of the tool was kept constant throughout the experiments by keeping the plunging depth of the tool shoulder fixed. Figure (3) shows friction stir welded specimens.

Tests and inspections

Tensile test was carried out on samples cut perpendicular to the welding direction to determine the tensile properties of the welded joints, where the size of the tensile specimens was carried according to ASTM B557M [13]. Tensile properties of each joint were evaluated at room temperature with full maximum capacity (50 KN) constant crosshead speed of 5mm/min using the computerized (Zwick/Roell 100 KN) Universal testing machine at the Materials Engineering Department at the University of Technology.

X-Ray diffraction tests were done in the Ministry of Science and Technology in Baghdad, with a supplied voltage of (40KV) and current of (20mA). The target is Copper with a wave length ($\lambda=1.5406 \text{ \AA}$) and the filter is Nickel.

Heat treatments were performed in the department of production and metallurgy engineering at University of Technology. An electric furnace was used for heat treatments. The specimens were heated to (495C°) stabilized at these temperatures for (30) minutes, quenched in water, then left 7 days in ambient air to obtain the natural ageing.

Hardness test Samples Preparation for Hardness the samples made from a cross section of the FSSW joints and base alloy were ground polished and etched and observed under optical microscope in sequences steps. Wet grinding operation with water was done by using emery paper of SiC with the different grits of (220, 320, 500, and 1000). Polishing process was done to the samples by using diamond paste of size ($1\mu\text{m}$) with special polishing cloth and lubricant. They were cleaned with water and alcohol and dried with hot air. The Vickers hardness tests were taken perpendicular to the welding direction by the digital micro Vickers hardness tester used under applied load (200 g). This test carried out in the Production and Metallurgy Engineering Department at University of Technology.

Bending fatigue tests, the fatigue tests were carried out in the Mechanical Engineering Department at the University of Technology.

A fatigue-testing machine of type Hi-Tech rotating bending was used to execute all fatigue tests with constant amplitude. The specimens were subjected to an applied load from the right side of the perpendicular to the axis of specimen, developing a bending moment. Therefore, the surface of the specimens is under tension and compression stresses when it rotates. Both similar and dissimilar joints samples were classified in three groups according to the position of the welding line with respect to point of the applied force. Figure (4) shows positions of the welding line in fatigue samples used in this work.

Results and Discussion

Tensile test results

Table (2) shows the values of the ultimate tensile stress (σ_{ULT}), yield stress (σ_Y), and elongation (EL) before and after the friction stir welding and heat treatment. It was seen that the welding efficiency (which will be defined as the ratio of the tensile strength of the weld to the base material tensile strength) was 62.8% for similar 2024-T3 joint; the reason is that, the weld nugget is composed of fine recrystallized grains, while the TMAZ is composed of coarse-bent recovered grains [14]. Therefore, the interface between the weld nugget and the TMAZ is clearly visible and becomes a weaker region or location in the joint and the joint is fractured at this interface during the tensile testing. Figure (5) shows FSW joints failed at heat affected zone (HAZ) of the advancing side (AS). The longitudinal samples extracted from the stir zone of dissimilar (2024T3-6061T6) welded samples have lower ultimate strength than similar welded (2024T3-2024T3) samples about 20.9%, because it is dominated by the weakest material strength and ductility, which was in this case 6061T6 as reported in Table (2).

For the post welding heat treatments similar 2024T3 samples, the results of the test showed that both strength and ductility of the welds increase after heat treatment, where the increase in the ultimate strength was 8.2%. The reason why the strength of the post welding heat treatments plates is less than that of the base metal is the coarsening and dissolution of the strengthening precipitates due to the thermal cycle of FSW [15]. After solution treatment, the strengthening precipitates dissolve into the matrix. The quenching process freezes the alloying elements in their supersaturated condition. When the welded plate is allowed to naturally age, then the strength of the welding will increase due to the re-precipitation of the alloying elements. The ductility does show a positive response.

X-Ray diffraction test

Residual stress data are presented as functions of distance from the weld centerline for both the as-welded condition and after the heat treatments. Compressive stresses are shown as negative values and tensile as positive see Figure (6). One can notice that the X-ray diffraction data shows that the plates, in the as welded 2020T3 have high tensile residual stresses because of the effect of heat rising during friction stir welding, maximum surface tension on the order of (140.72 MPa) occurs at the shoulder outside edge, which is believed to be caused by the high temperature gradient and high shear force by the shoulder periphery edge in this region. In the dissimilar 2024T3-6061T6 joint, it is found that the tensile residual stress higher than that of similar materials joint because of aluminum alloy 6061T6 more affected with heat rising than 2024T3, where the maximum tensile residual stress in this type is about 441.27MPa.

For the post welding heat treatment pieces, there is a decrease in tensile residual stresses (about 56.4 % reduction from the as-welded joint in the stirred zone) due to stress relief resulting in strengthen the welded joint. Generally, welding causes the highest tensile residual stresses, and heat treatments results in reduces these stresses.

Micro-hardness results

The welding process affected the micro-hardness values by reducing them significantly. Figure (7) shows the Hardness distribution in similar 2020T3 joints, dissimilar 2024T3-6061T6 joint, and post welding heat treatment 2024T3 joints. For the similar 2024-T3 joints, The hardness of the 2024-T3 base metal was recorded to be about (160 HV), while the minimum hardness recorded for the HAZ was about (103.7 HV) which accounts about 64.8% of the base metal, and the hardness recorded for the NZ was about (112 HV) which account about 70% of the base metal. This difference was due to the amount of heat generated in the welded zone which caused softening of the nugget, TMAZ, and HAZ due to dissolution and coarsening of the strengthening precipitates during the welding process [16]. Such hardness profile correlates with the point of rupture of the samples in the tensile test. The decreasing in the weld hardness can be attributed to the dissolution of precipitates and subsequently the weld cooling rates do not favor nucleation and growth of all precipitates [17]. In the HAZ precipitates are not dissolved in the matrix, and consequently there is no reappearance of precipitates due to post weld thermal cycle. This causes the lowest hardness and consequently fractures during tensile testing in the HAZ and that conform to [18].

Dissimilar welds hardness profile for 6061T6-2024T3 with 6061T6 at the advancing side present two half-W shape. One side globally corresponds to a half of a 2024T3-2024T3 similar weld, while the other side globally corresponds to a half of a 6061T6-6061T6 similar weld. The transition between both sides occurs in the nugget, whose hardness depends on its composition. A nugget zone composed of a mixing of both alloys presents hardness variations. The results indicated that the microhardness in the 6061T6-2024T3 joint was lower than that in the 2024T3-2024T3 at the NZ, the ratio of decreasing microhardness was 6.4%.

For the post welding heat treatment 2024T3-2024T3, the hardness is higher than as welded alloys by increasing 29.4% in the nugget zone, 29.98% in the TMAZ, and 28.2% in the HAZ because that the strength of the welds increases due to the re-precipitation of the alloying elements as a result of water quenching and natural ageing.

Fatigue test results

The S-N curves for the 2024T3 base material was shown Figure (8), when the value of bending stress was decreased, the number of cycles increase and the life of the sample at (338.6 MPa) was (116207 cycle). It was observed that the life would be more than 10^5 cycle when the applied bending stress was (196.75 MPa) without failure.

The fatigue life of similar 2024-T3 FSW joints was lower than those of the base materials as shown in Figure (8). Generally, FSW material exhibits lower strength and ductility properties than the base material [8]. This is due to the softening in the SZ resulted from the deterioration of precipitates [10].

The results show that there are major differences in fatigue behaviors between the FSW specimens in different welding positions for similar welding joints Figure (8). Where, for the welding position at a distance D equal $0.35L$ from the loading end, the fatigue life is less than those of 2024T3 base material by 45%, while for welding line at distance $0.7 L$ from the same end, the decrease in fatigue strength was 56% from the 2024T3 base material in a 10^6 cycle. The reason of this difference in fatigue resistance is the difference in moment lever of the two points and this due to increase the bending moment in a point of distance $0.7L$ because of the larger moment lever when compared with a point at a distance $0.35 L$. This effect was maximized in case of welding line at distance L (at the fixing point); it is found that its fatigue life was much lower than the other cases and the maximum number of cycles don't exceed 628650 cycle in a smallest applied stresses values (45.75MPa), i.e. reduction in the fatigue strength reaches to 71% from the 2024T3 base material in 628650 cycle.

When comparing with similar joints, it is found that the fatigue resistance of the dissimilar joints was lower than fatigue resistance for the similar joints in all welding position this is due to the alternate lamellar structure in the nugget zone, as shown in Figure (9). For the dissimilar joints as shown in Figure (10), the reduction in fatigue resistance from the 2024T3 base material was 58% for welding line at D equal to $0.35 L$ and 67% for welding line at D equal to $0.7 L$ in 10^6 cycle. While, for the welding line at the fixing point, the fatigue resistance was very low and the maximum number of cycles was about 254740 cycle at stress equal to (35.875 MPa) i.e. reduction in the fatigue strength reaches to 70% from the 2024T3 base material in 254740 cycle.. The cause for these differences was the same reason for the fatigue resistance

differences in the similar welded joints. These results showed that the position of the welding line was effect on the fatigue behavior in both the similar and dissimilar joints.

The effect of heat treatments on the FSW plates was showed in Figure (11), however in the low-cycles regime; the difference in fatigue resistance between the as-welded samples and post welding heat treatments samples for the similar 2024T3 joints is not clear while the difference increase in high cycles regime, where the increase in fatigue resistance was about 31% in 10^6 cycle more than non heat treatments of the similar 2024T3 joint at 0.7L. The fatigue strength of the welded plates with heat treatments is apparently lower than that of the 2024T3 base material by 25 % in 10^6 cycle, this is because the hardness increment resulted from this type is not much large and the tensile residual stresses induced by welding process were not removed permanently by the heat treatments. Meanwhile in the high-cycle regime, consequently the fatigue strength of the FSW was remarkably improved by the heat treatments. As expected, a smoother surface in similar 2024T3 alloy has a visible influence on the fatigue strength see Figure (12), since surface defects inducing notch effects are avoided in this way, the decrease in fatigue life was about 66 % from the 2024T3 base material (24% less than the finishing samples) in 10^6 cycle. Because surface skimming was applied and eliminated stress concentration arising from profile irregularities such as tool marks and weld flashes. The fatigue curve equations and fatigue reduction ratios for the welding cases are listed in Table (3). By comparing the value of fatigue endurance limit in each case with that of the base metal, we showed that the minimum value of fatigue reduction ratios was for the post welding heat treatments samples, which gives a clear indication that there is improvement in fatigue endurance limit by the heat treatments compared with other cases.

CONCLUSIONS

1. The FSW is a process suitable to weld the aluminum alloy 2024T3 that is not weldable and the welding efficiency achieves about 62.8% of the ultimate tensile strength.
2. Fatigue strength at 10^6 cycles depend strongly on welding line position where for welding line at a distance 0.35L from loading side, the reduction in fatigue limit with respect to 2024T3 base material was 45% for similar joint and 58% for dissimilar joints, and for welding line at a distance 0.7 L, the reduction in fatigue strength was 56% for similar joint and 67% for dissimilar joints. While, it was a large reduction in the fatigue strength reaching to 70% in both similar and dissimilar joint for the welding joint at a distance L (i.e at the fixing end).
3. The post welding heat treatments has a large effect on the mechanical properties where it improved tensile stress, micro hardness, and the fatigue life of the joint by 7.77 %, 29.4 %, and 31%, respectively. The improvement done by reducing the amount of residual stresses generating during the welding process (about 56.4 % reduction in the stirred zone).
4. There is a reduction in fatigue endurance limit about 10% for the non-finishing samples of the similar 2024T3 joint less than the welded finishing

samples which assures that the softening and polishing processes improved the fatigue endurance limit of the FSW joints.

REFERENCES

- [1] Flores OV, Kennedy C, Murr LE, Brown D, Pappu S, and Nowak BM, "Microstructural issues in a friction-stir-welded aluminum alloy", *Scripta Mater*;38(5):pp.703–8, 1998.
- [2] Friction Stir Link Inc, available at [http://www.frictionstirlink.com /fslfswdescription.html](http://www.frictionstirlink.com/fslfswdescription.html).
- [3] A. Cirello, "AA6082_T6 friction stir weld joints fatigue resistance: influence of process parameters", pp.805, 2006.
- [4] Shusheng Di , Xinqi Yang , Guohong Luanb, and Bo Jian, "Comparative study on fatigue properties between AA2024-T4friction stir welds and base materials", *Materials Science and Engineering, A* 435-436, pp. 389-395, 2006.
- [5] Moreira, Jesus, Ribeiro, and Castro, "Fatigue crack _growth behavior of the friction stir welded 6082_T6 aluminum alloy", *Mecânica Experimental*, Vol.16, pp.99-106, 2008.
- [6] P. Cavaliere, A. De Santis, F. Panella, and A. Squillace, "Effect of welding parameters on mechanical and microstructural properties of dissimilar AA6082–AA2024 joints produced by friction stir welding", *Materials and Design* 30, pp.609-616, 2009.
- [7] O. Hatamleh, "Fatigue Crack Growth of Preened Friction Stir _Welded _7075 Aluminum Alloy under Different Load Ratios", *Journal of materials engineering and performance*, published online, 2009.
- [8] H. Aydın, A. Bayram, A. Uğuz, and K. S. Akay, "Influence of Welding Parameters on the Fatigue Behavior of Friction Stir Welds of 3003-O Aluminum Alloys", *ISSN 1392–1320 MATERIALS SCIENCE (MEDŽIAGOTYRA)*, Vol. 16, No. 4, pp. 311-319, 2010.
- [9] A.M. Abdullah, "Fatigue Properties OF Friction stir Welded Alluminum Alloy", MS.C. Thesis, Al-Nahrain University, 2011.
- [10] Y. Sano, K. Masaki, T. Gushi, and T. Sano, "Improvement in fatigue performance of friction stir welded A6061-T6aluminum alloy by laser peening without coating", *Materials and Design* 36, pp.809–814, 2012.
- [11] N. A. Hamoody, "Effect of Friction Stir Welding and Process Parameters on the Mechanical Properties of 2024T3 Aluminum Alloy Weldments", PhD. Thesis, University of Technology, 2012.
- [12] M. A. Muhammed, "The Effect of Friction Stir Welding on the Mechanical Properties of AA 7020-T53", PhD. Thesis, Al-Nahrain University, 2012.
- [13] Annual Book of ASTM Standards, "Metal Test Methods and Analytical Procedures", American Society for Testing and Material, Volume 03.01, Section3, pp52-62, pp.462 – 475, 1988.
- [14] H.J. Liu, H. Fujii, M. Maeda, and K. Nogi, "Tensile properties and fracture locations of friction-stir-welded joints of 2017-T351 aluminum alloy", *Journal of Materials Processing Technology* 142, pp.692–696, 2003.
- [15] A.A. Zadpoor and J. Sinke, "Effects of Post-Weld Heat Treatment on the Mechanical Properties of Similar- and Dissimilar-Alloy Friction Stir Welded Blanks", *Journal of Materials Science and Engineering*, pp.1315- 929, 2011.

- [16] T. S. Srivatsan, S. Vasudevan, and L. Park, “The Tensile Deformation and Fracture Behavior of Friction Stir Welded Aluminum Alloy 2024”, Journal of Materials Science and Engineering A 466, pp. 235-245, 2007.
- [17] T. Venugopal, K.S. Roa , and P. Roa, “Studies on Friction Stir Welded AA7075-T6 Aluminum Alloy”, Trans. Indian Inst. Met., Vol. 57, No. 6, pp. 659-663, 2004.
- [18] K. Kumar and S.V. Kailas, "The role of friction stir welding tool on material flow and weld formation", Materials Science and Engineering, pp. 367-374, 2007.

NOTATIONS

<u>Symbols</u>	<u>Definition</u>
AS	Advanced side
B.M	Base material
D	Distance from the applied force point on (mm)
EL	Elongation
FSW	Friction stirs
F _s	Friction stirs
HAZ	Heat affected zone
HV	Vickers hardness
NZ	Nugget zone
N	Number of Cycles
PWHT	Post welding heat treatments
R	Stress Ratio
S	Stress (MPa)
TMAZ	Thermo mechanical affected zone
σ_{ULT}	Ultimate tensile strength (MPa)
σ_y	Yield stress (MPa)

Table (1): Aluminum alloys chemical composition

Elements		%Si	%Fe	%Cu	%Mn	%Mg	%Zn	%Cr	Others%	%Al
Materials										
AA 2024T3	Nominal composition	0.5 max.	0.5 max.	3.8-4.9	0.3-0.9	1.2-1.8	0.25	0.1	0.3	Bal.
	Actual composition	0.121	0.265	3.8	0.511	0.134	0.134	0.009	0.026	Bal.
AA 6061T6	Nominal composition	0.4-0.8	0.7 max	0.15-0.4	0.15	0.8-1.2	0.25 max	0.04-0.35	0.3	Bal.
	Actual composition	0.614	0.444	0.368	0.08	0.004	0.004	0.068	0.0281	Bal.

Table (2): Results of tensile test for heat treatment series

Type of Series	σ_y (MPa)	σ_u (MPa)	El%
2024T3	322	487	15
6061T6	298	345	12
2024T3-2024T3	269	306	0.92
2024T3-6061T6	239	242	0.84
2024T3 PWHT	286	319	1.8

Table (3) :Fatigue curve equations and fatigue reduction ratios

Welding condition	Fatigue curve equations	Fatigue endurance limit	Reduction in fatigue endurance limit with respect to 2024T3BM
2024T3 B.M	$\sigma = 6028.4Nf^{-0.245}$	204.27	-
Sim 0.35L	$\sigma = 8844.3Nf^{-0.316}$	112.37	45%,
Sim 0.7L	$\sigma = 4025.8Nf^{-0.275}$	90.11	56%
Sim L	$\sigma = 6237.9Nf^{-0.35}$	58.29	71%
Dis 0.35L	$\sigma = 2407.5Nf^{-0.241}$	86.19	58%
Dis 0.7L	$\sigma = 8309.6Nf^{-0.348}$	67.85	67%
Dis L	$\sigma = 3388.2Nf^{-0.322}$	61.92	70%
PWHT(2024T3 at 0.7L)	$\sigma = 1093.5Nf^{-0.142}$	153.75	25 %
W.F(2024T3 at 0.7L)	$\sigma = 6825.3Nf^{-0.333}$	68.57	66 %

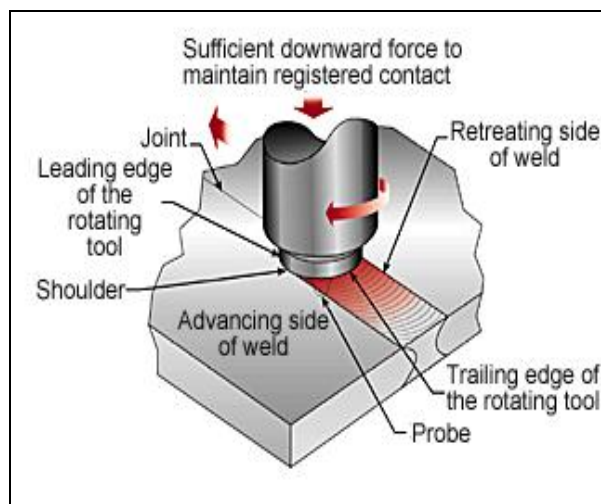


Figure (1) Schematic diagram of the FSW process [2]



Figure (2) Tool geometry used in present work



a- Similar 2024T3 joint



b- Dissimilar 2024T3-6061T6 joint

Figure (3) Welded friction stir welded specimens

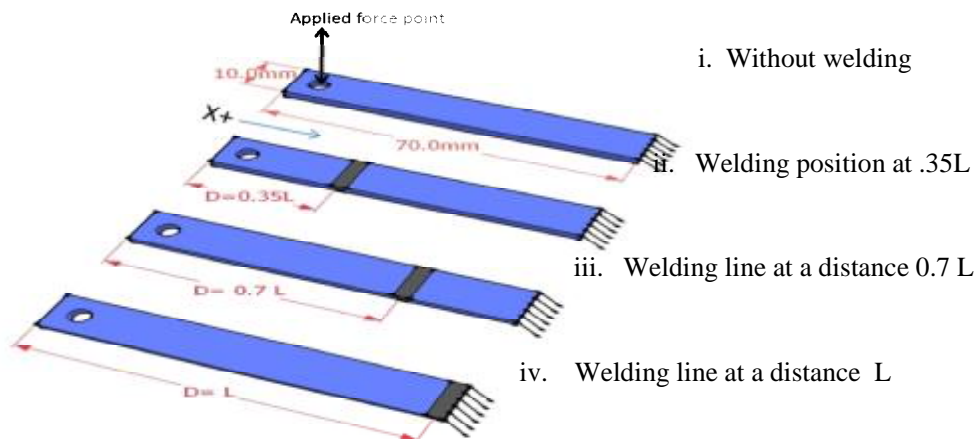


Figure (4) Fatigue test samples with welding line at different positions.

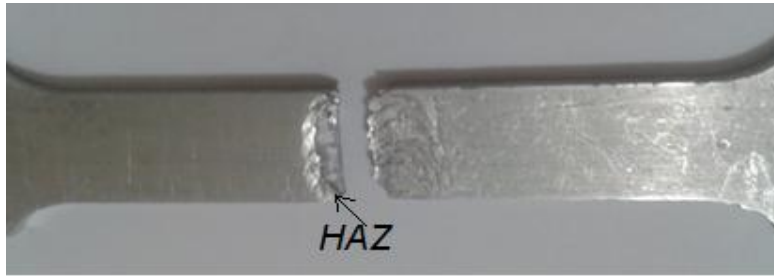


Figure (5) FSW joints failed at heat affected zone (HAZ) of the advancing side (AS)

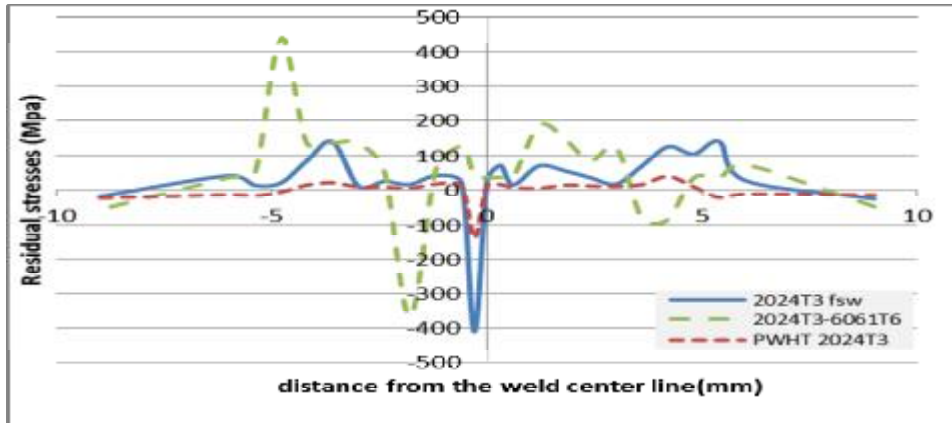


Figure (6) Residual stress perpendicular to the weld line in FSW for similar joint materials with and without heat treatments and for dissimilar joint materials .

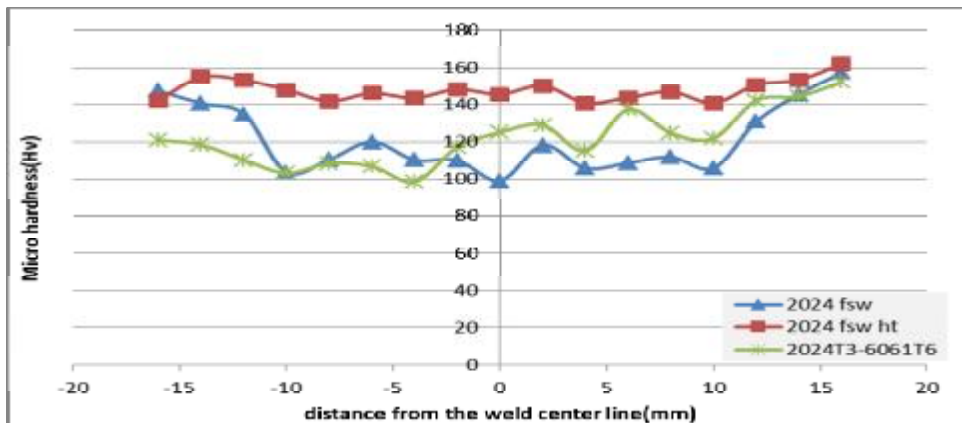


Figure (7) Hardness distribution in similar 2020T3 joints, dissimilar 2024T3-6061T6 joint, and post welding heat treatment 2024T3 joints.

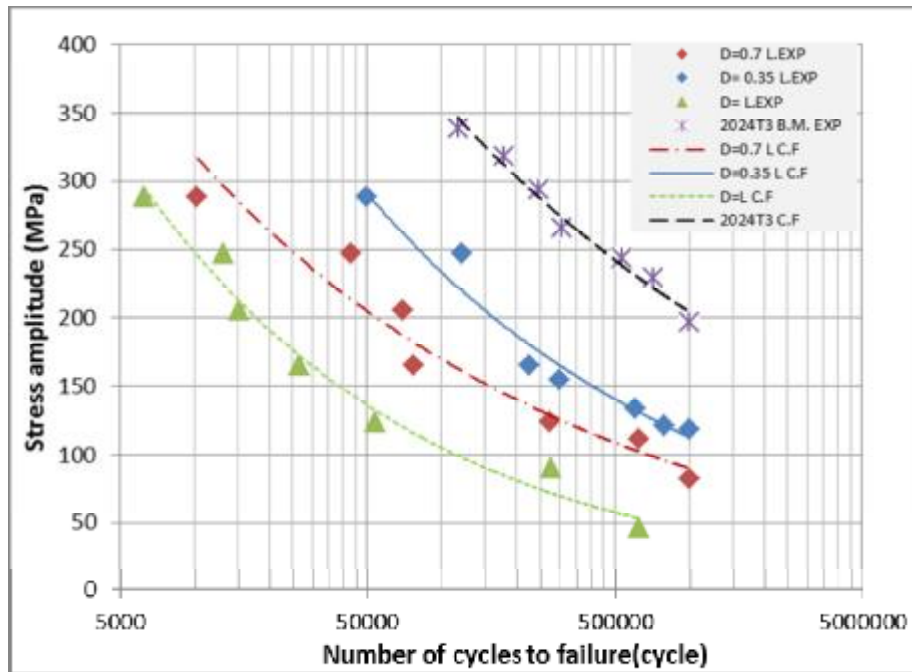


Figure (8) Fatigue curves for similar 2024T3 joints at different welding positions and 2024T3 B.M

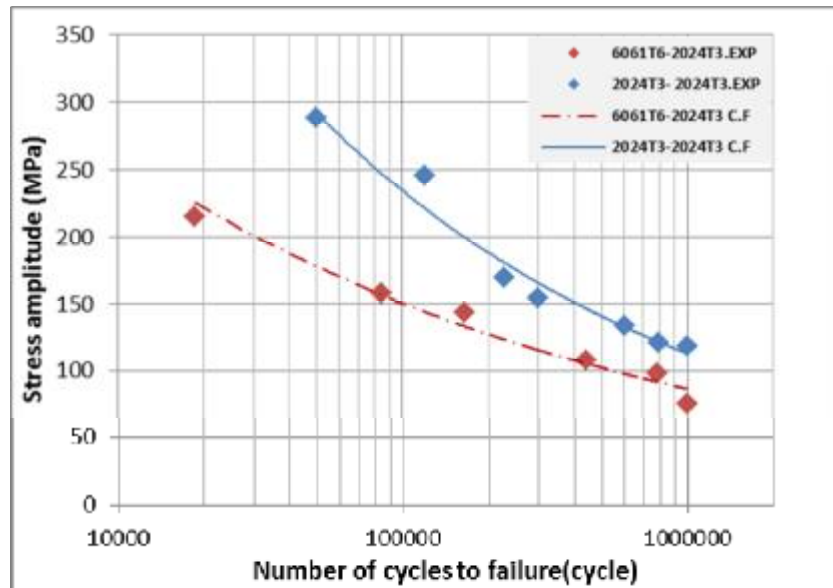


Figure (9) Comparison between S-N curves for similar 2024T3 joints and dissimilar 2024T3-6061T6 joints at 0.35L

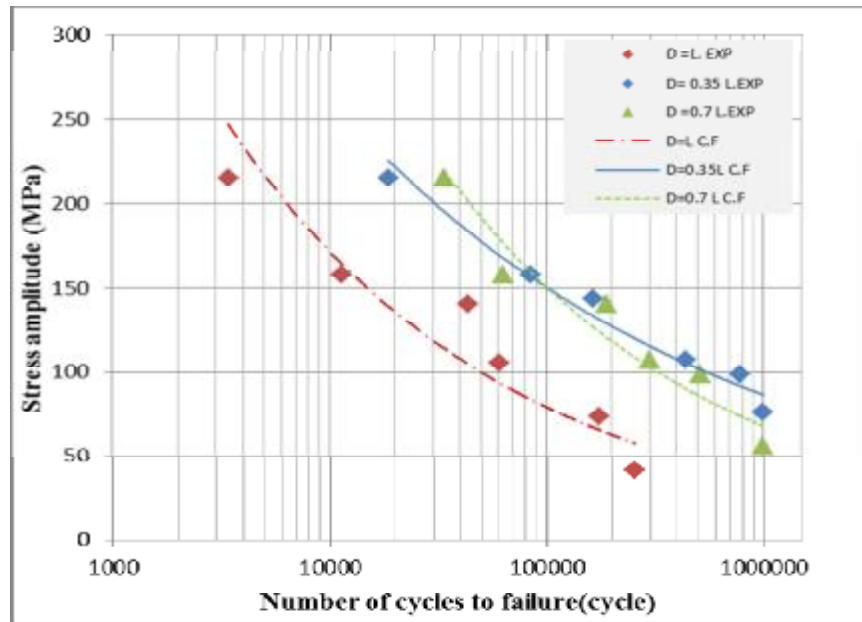


Figure (10) S-N curves for dissimilar 2024T3-6061T6 joints at different welding positions

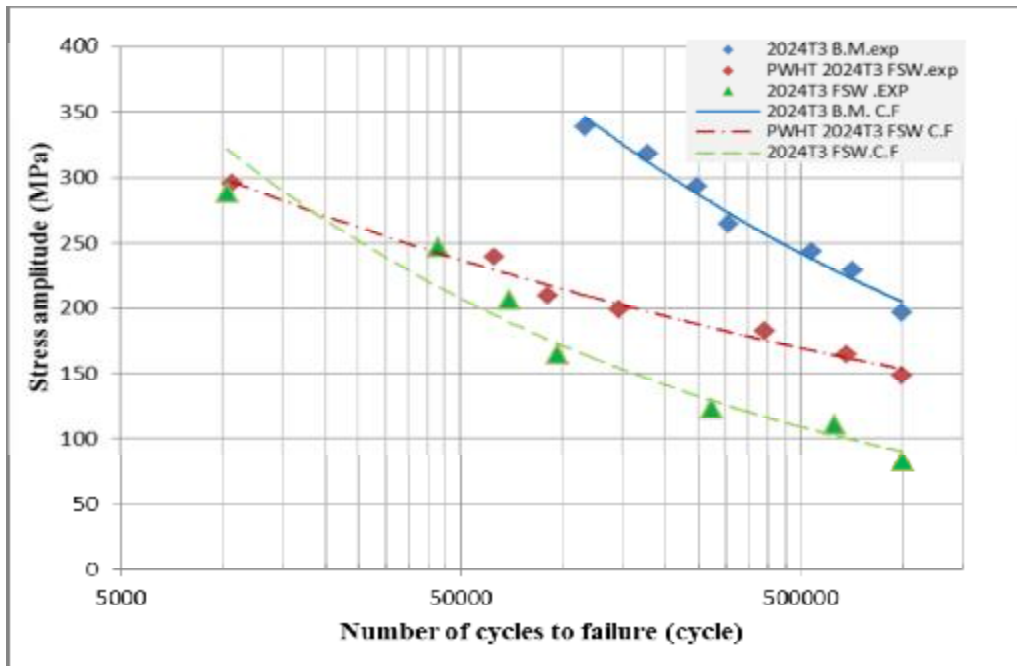


Figure (11) Effect of post welding heat treatment on the fatigue performance

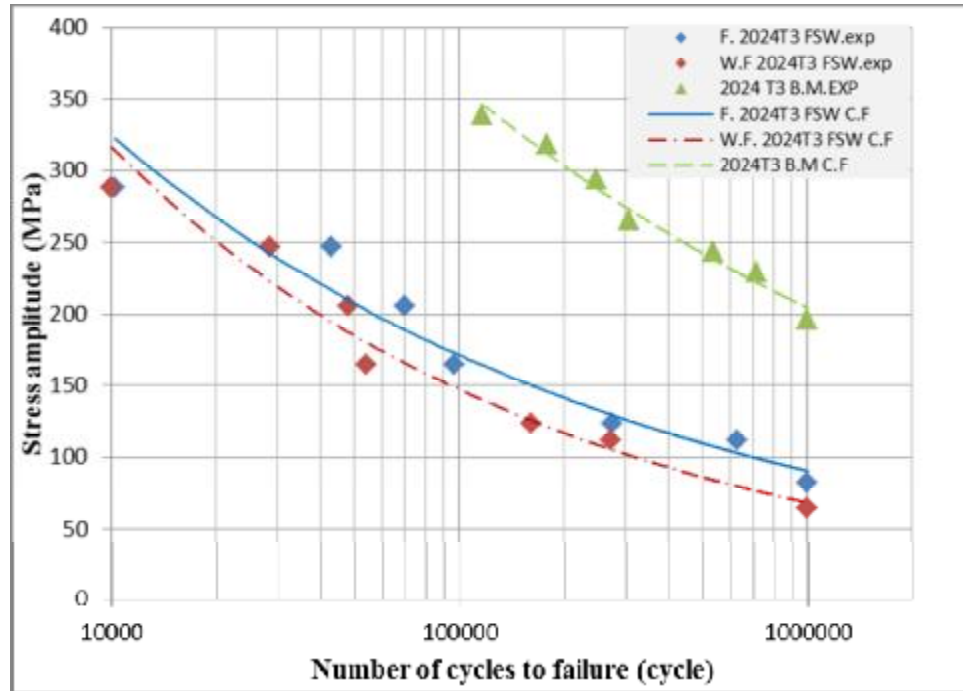


Figure (12) Effect of softening and polishing on the fatigue performance